Journal of Hazardous Materials 186 (2011) 699–706

Contents lists available at ScienceDirect

Journal of Hazardous Materials

journal homepage: www.elsevier.com/locate/jhazmat

Removal of pyridine from liquid and gas phase by copper forms of natural and synthetic zeolites

Mária Reháková[a,*], Ľubica Fortunová[a], Zdeněk Bastl[b], Stanislava Nagyová[c], Silvia Dolinská[d], Vladimír Jorík[e], Eugen Jóna[f]

[a] Institute of Chemistry, Faculty of Science, P.J. Šafárik University, 041 54 Košice, Slovak Republic
[b] J. Heyrovsky Institute of Physical Chemistry, ASCR, v.v.i., 18223 Prague 8, Czech Republic
[c] Department of Physics, Electrotechnical Faculty, Technical University, 042 00 Košice, Slovak Republic
[d] Institute of Geotechnics, Slovak Academy of Sciences, 043 53 Košice, Slovak Republic
[e] Department of Inorganic Chemistry, Faculty of Chemical and Food Technology, Slovak University of Technology, 81237 Bratislava, Slovak Republic
[f] Department of Chemistry and Technology of Inorganic Materials, Faculty of Industrial Technologies, Trenčín University of Alexander Dubček, 02032 Púchov, Slovak Republic

ARTICLE INFO

Article history:
Received 16 March 2010
Received in revised form 8 November 2010
Accepted 12 November 2010
Available online 20 November 2010

Keywords:
Natural zeolite
Clinoptilolite
ZSM5
Copper
Pyridine

ABSTRACT

Zeoadsorbents on the basis of copper forms of synthetic zeolite ZSM5 and natural zeolite of the clinoptilolite type (CT) have been studied taking into account their environmental application in removing harmful pyridine (py) from liquid and gas phase. Sorption of pyridine by copper forms of zeolites (Cu-ZSM5 and Cu-CT) has been studied by CHN, X-ray photoelectron spectroscopy, X-ray powder diffractometry, FTIR spectroscopy, thermal analysis (TG, DTA and DTG) and analysis of the surface areas and the pore volumes by low-temperature adsorption of nitrogen. The results of thermal analyses of Cu-ZSM5, Cu-$(py)_x$ZSM5, Cu-CT and Cu-$(py)_x$CT zeolitic products with different composition (x depends on the experimental conditions of sorption of pyridine) clearly confirmed their different thermal properties as well as the sorption of pyridine. In the zeolitic pyridine containing samples the main part of the pyridine release process occurs at considerably higher temperatures than is the boiling point of pyridine, which proves strong bond and irreversibility of py–zeolite interaction. FTIR spectra of Cu-$(py)_x$zeolite samples showed well resolved bands of pyridine. The results of thermal analysis and FTIR spectroscopy are in a good agreement with the results of other used methods.

1. Introduction

The compounds of pyridine occur in the environment as effluents from different industries such as pharmaceuticals, dyes, herbicides and pesticides manufacturing, shale oil processing, food processing and coal carbonization [1,2]. Pyridine is there used as a solvent, intermediate and also as a catalyst. Pyridine is a volatile liquid with a threshold odor concentration of 0.1 ppm (58.6 mg L^{-1}) and an odor index of 2390 [3,4]. According to USEPA pyridine is a toxic, carcinogenic and teratogenic compound rated as a priority pollutant [4,5]. Therefore, exposure to pyridine-laden emissions may have severe health implications. Conventionally, the emissions, contaminated wastewaters or industrially contaminated soil containing pyridine are treated by different physico-chemical methods such as adsorption [6,7], chemical oxidation, incineration or biodegradation [1–5,8–10]. However, most of these treatment methods are costly and energy claiming.

Zeolitic materials are used to decrease the residual content of heavy metals and other toxic compounds in wastewaters and industrially contaminated soil [11–18]. The natural zeolite of the clinoptilolite type as well as synthetic zeolite ZSM5 look to be very interesting for the removal of pyridine due to their sorption characteristics resulting from a combination of ion-exchange and molecular sieve properties, which can be relatively easily modified.

The aim of our present study was the sorption of pyridine from a liquid and gas phase by copper forms of synthetic zeolite ZSM5 (Cu-ZSM5) and natural zeolite of clinoptilolite type (Cu-CT). The obtained zeolitic products containing pyridine were characterized by CHN, X-ray photoelectron spectroscopy, X-ray powder diffractometry, FTIR spectroscopy, thermal analysis – TG, DTA and DTG and analysis of the surface areas and the pore volumes by low-temperature adsorption of nitrogen.

2. Experimental

2.1. Chemicals and materials

A synthetic zeolite Na-ZSM5 (Slovnaft a.s. Bratislava) of the chemical composition (without water): 2.683% Na_2O, 0.528% CaO,

* Corresponding author.
E-mail address: maria.rehakova@upjs.sk (M. Reháková).

0304-3894/$ – see front matter © 2010 Elsevier B.V. All rights reserved.
doi:10.1016/j.jhazmat.2010.11.051

3.717% Al_2O_3, 93.072% SiO_2 (ratio SiO_2/Al_2O_3 = 42.94) and natural zeolite of the clinoptilolite type from the Eastern Slovakian deposit at Nižný Hrabovec with content of clinoptilolite 84% and the chemical composition (without water): 65.0–71.3% SiO_2, 11.5–13.1% Al_2O_3, 2.7–5.2% CaO, 2.2–3.4% K_2O, 0.7–1.9% Fe_2O_3, 0.6–1.2% MgO, 0.2–1.3% Na_2O, 0.1–0.3% TiO_2 (ratio SiO_2/Al_2O_3 = 4.8–5.4) [12] have been used in our study.

Na-ZSM5 was thermally activated for 3–4 h by heating at continuously increasing temperature in the range from 150 to 400 °C (1 h at 400 °C). Natural zeolite of the clinoptilolite type was thermally activated for 2 h by heating at temperature 110 °C. Based on our long-term experimental experience the thermal activation of natural zeolite was realized at lower temperature and shorter time than the thermal activation of synthetic ZSM5 [19,20]. The temperature and time of the thermal activation proved to be sufficient in such case if, after the thermal activation, the modification is realized using aqueous solution.

Copper sulphate, pyridine and other chemicals were of p.a. purity (Merck).

2.1.1. Material preparation

Copper forms of synthetic zeolite ZSM5 and natural clinoptilolite were prepared by a reaction of thermally activated Na-ZSM5 and natural clinoptilolite with $CuSO_4$ solution of concentrations 0.1 and 1.0 mol dm^{-3}. After 2 h of stirring the heterogeneous mixtures were several times decanted and centrifuged in order to get them rid of sulphate ions, and then dried for 2 h at 90–100 °C. The copper forms were denoted as Cu-ZSM5 and Cu-CT, marked by (0.1 M) or (1 M) denotation according to the solution concentration used.

Prepared copper forms of ZSM5 and clinoptilolite were used for sorption of pyridine from liquid as well as gas phase.

The products obtained by sorption of pyridine from liquid phase were prepared from copper forms of zeolites (6 g) by adding pyridine in liquid phase: 10 ml for Cu-ZSM5, 8 ml for Cu-CT (it was necessary to use the higher volume of pyridine for the Cu-ZSM5 sample to cover all surface). The heterogeneous mixtures were left to stand for 1 h (with occasional mixing), decanted several times and centrifuged. The final products were dried in a dark desiccator over silica gel at room temperature. The products were denoted as Cu-py-ZSM5 (L) and Cu-py-CT (L).

The products obtained by sorption of pyridine from gas phase were prepared by exposing a layer of copper forms Cu-ZSM5 and Cu-CT (5 g) to pyridine vapours for 10 days at room temperature in a dark desiccators. Thus obtained samples were left in the desiccator without pyridine for the next three days. The products were denoted as Cu-py-ZSM5 (G) and Cu-py-CT (G).

2.2. Methods

CHN elemental analyses were performed by a PerkinElmer 2400 Elemental Analyser. The copper and other elements were determined by the X-ray photoelectron spectroscopy (XPS).

The X-ray photoelectron spectra (XPS) were obtained with high resolution electron spectrometer ESCA 310 (Gammadata Scienta, Sweden) equipped with rotating anode of special UHV design. Photoelectrons were excited using monochromatized Al K_α X-rays ($h\nu$ = 1486.6 eV), eliminating thus the bremsstrahlung radiation which might cause reduction of Cu^{2+} species. The samples were spread on gold plates which were mounted on a sample probe by means of tantalum clips. Detailed spectral scans were taken over Cu (2p), Si (2p), O (1s), C (1s) and N (1s) spectral regions. The instrument was calibrated so that the difference between Au $4f_{7/2}$ photoelectron peak and Fermi level was 84.0 eV. The spectrometer was operated in the fixed analyser transmission mode. The background pressure of the residual gases during spectral accumulation was typically of the order of $\sim 10^{-7}$ Pa. The Si (2p) binding energy (103.4 eV) was used as internal standard in calibration in order to compensate for static surface charging of the sample. The XPS measurements were carried out on the samples in the as-received state. The peak positions and areas were determined by fitting the unsmoothed experimental data after subtraction of the Shirley [21] background. Quantification of the element surface concentration ratios was accomplished by correcting the integral intensities of the photoemission peaks for their cross-sections [22] and accounting for the dependence of the analyser transmission [23] and electron mean free paths on kinetic energy of electrons [24]. Core level binding energies were determined with an accuracy of ±0.2 eV. The results obtained did not depend on the angle of electron detection, indicating thus the absence of measurable surface concentration gradients.

Infrared spectra were obtained with KBr disc technique in the range 400–4000 cm^{-1} using AVATAR 330 FTIR Thermo Nicolet IR spectrometer.

The thermal analyses TG, DTA and DTG were measured up to 800 °C in air on a NETZSCH STA 409 PC/PG under the conditions: sample weight 25 mg, heating rate 10 °C/min, Al_2O_3 crucible.

X-ray powder diffraction patterns were recorded with Bragg-Brentano diffractometer Philips PW 1730/1050, using β-filtered Co K_α radiation, 40 kV/35 mA in the range of 2θ 3–71°, step 0.02°.

The analysis of surface areas and the pore volumes of the zeolitic samples were realized by a GEMINI 2360 (Micrometrics, USA). The specific surface area was determined by low-temperature adsorption of nitrogen. Before the measurements, the samples were heated for 2 h at 105 °C.

3. Results and discussion

The zeoadsorbents on the basis of copper forms of synthetic zeolite ZSM5 and natural zeolite of the clinoptilolite type were used for removal of toxic pyridine from the liquid and gas phase based on ion-exchange and sorption properties of zeolites. In the first step, copper forms of synthetic ZSM5 and natural clinoptilolite (Cu-ZSM5, Cu-CT) were obtained by an ion-exchange mechanism of zeolites with copper sulphate solution, starting from Na-ZSM5 and natural zeolite of the clinoptilolite type. In the second step, the copper forms of synthetic and natural zeolites were used for the sorption of pyridine from the liquid and gas phase. In different experimental conditions, zeolitic products with different content of pyridine were obtained. The reaction of Cu-ZSM5 and Cu-CT with pyridine gave a blue-violet zeolitic product denoted as Cu-$(py)_x$ZSM5 and Cu-$(py)_x$CT (x depends on the experimental conditions of sorption of pyridine). The blue-violet colour of the products is given by the experimental conditions of sorption of pyridine as well as by the pyridine content. The copper forms of both zeolites containing pyridine and the starting samples Cu-ZSM5 and Cu-CT were analyzed by the CHN, XPS, XRD, FTIR spectroscopy, thermal analysis – TG, DTG, DTA and determination of the surface areas and the pore volumes by low-temperature adsorption of nitrogen.

The presence of copper in all products, in the starting materials Cu-ZSM5, Cu-CT as well as in the pyridine containing products Cu-$(py)_x$ZSM5 and Cu-$(py)_x$CT was confirmed by XPS analyses. The results of CHN analyses, XPS and thermal analyses checked the presence of pyridine after its sorption by copper forms of synthetic ZSM5 and natural clinoptilolite. The results of the CHN analyses were in a good agreement with the results of thermal analyses.

The comparison of the sorption ability of the copper forms of synthetic zeolite ZSM5 and natural zeolite CT showed that the synthetic zeolite sorbed more pyridine than the natural CT. More pyridine was sorbed from the gaseous emissions than from the liquid phase. The differences were caused by the fact that,

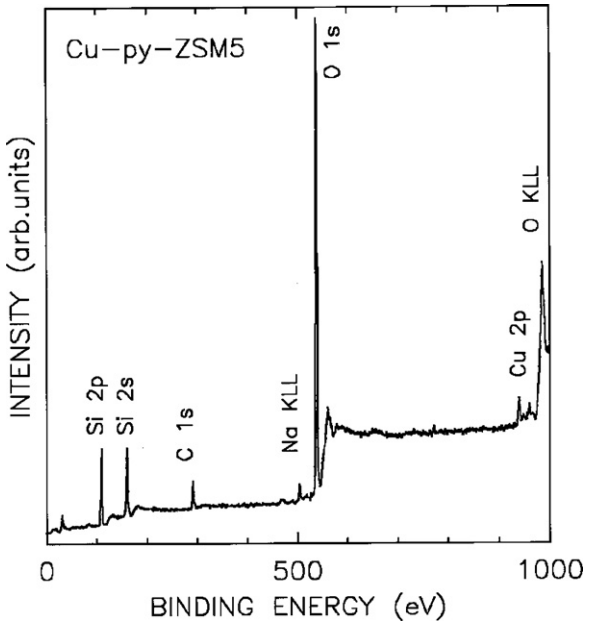

Fig. 1. Survey spectrum of the sample Cu-py-ZSM5 (L).

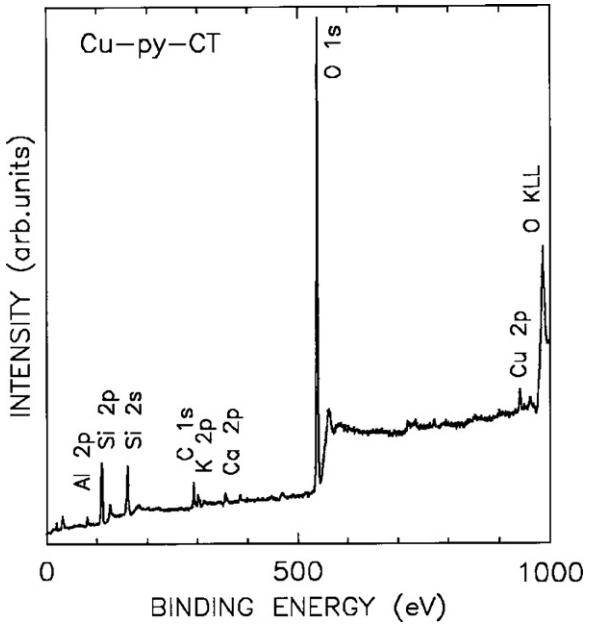

Fig. 2. Survey spectrum of the sample Cu-py-CT (L).

following the sorption from the liquid phase, the products were washed, unlike in the sorption from the gaseous phase. Consequently, a small part of pyridine in the products Cu-py-ZSM5 (G) and Cu-py-CT (G) could be sorbed physically on the surface.

For the preparation of the copper forms of zeolitic products two different concentrations of $CuSO_4$ solution were used: 0.1 and 1.0 mol dm^{-3}. The copper forms prepared with the higher 1.0 mol dm^{-3} concentration – CuCT (1 M) – of the starting solution sorbed by 0.5% more pyridine as compared with CuCT (0.1 M). The average content of pyridine in the zeolitic products after the pyridine sorption was as follows: Cu-py-ZSM5 (L) 5.5%, Cu-py-ZSM5 (G) 8%, Cu-py-CT (L) 3% and Cu-py-CT (G) 4%.

3.1. X-ray photoelectron spectroscopy

Using XPS spectroscopy the samples Cu-py-ZSM5 (L) and Cu-py-CT (L) were studied. The results obtained for Cu-ZSM5 sample were reported in our previous paper [25].

The XPS survey spectra with peak assignments are displayed in Figs. 1 and 2. The composition of superficial layers calculated from the integrated intensities of Si (2p), O (1s), N (1s) and Cu (2p) photoemission lines is summarized in Table 1. The concentrations of Al and K for Cu-py-CT (L) sample are also included. In Table 2 the core level binding energies and full widths at half maxima (FWHM) are given.

The intense satellite structure of Cu ($2p_{3/2}$) line characteristic of Cu(II) indicates (Fig. 3) that divalent copper dominates in the samples measured. The analysis of the spectra shows that in the sample Cu-py-ZSM5 (L) almost all copper is present in oxidation state Cu(II) while about 15% of Cu(I) is present in Cu-py-CT (L) sample. During spectra acquisition slow reduction of Cu(II) to Cu(I) accompanied by decrease of satellite intensity was observed (Figs. 4 and 5). To avoid significant reduction in measuring the spectra of a given sample we always started with Cu (2p) line. The partial reduction of Cu^{2+} ions to Cu^{+} in ZSM-5 and Y zeolites occurring under X-ray radiation has already been reported in the literature [26].

The N (1s) spectra of both studied samples (Fig. 6) are consistent with the presence of two different chemical states of nitrogen that can be assigned to nitrogen atoms associated with different surface sites [27,28].

Table 1
Surface concentrations of elements calculated from XPS data for the samples after sorption of pyridine.

Sample	Si	O	Cu	N	Al	K
Cu-py-ZSM5 (L)	1.00	2.03	0.031	0.013	–	–
Cu-py-CT (L)	1.00	2.42	0.027	0.016	0.39	0.05

Table 2
Core level binding energies of Si (2p), O (1s), N (1s) and Cu ($2p_{3/2}$) electrons and widths of the lines at half-heights (in parentheses). All values are in eV.

Sample	Line			
	Si (2p)	Cu ($2p_{3/2}$)	O (1s)	N (1s)
Cu-py-ZSM5 (L)	103.4 (2.5)	934.6 (4.0)	532.4 (2.6)	399.1 (2.1) 401.2
Cu-py-CT (L)	102.8 (2.6)	934.3 (4.8)	532.0 (2.8)	399.4 401.4 (2.1)

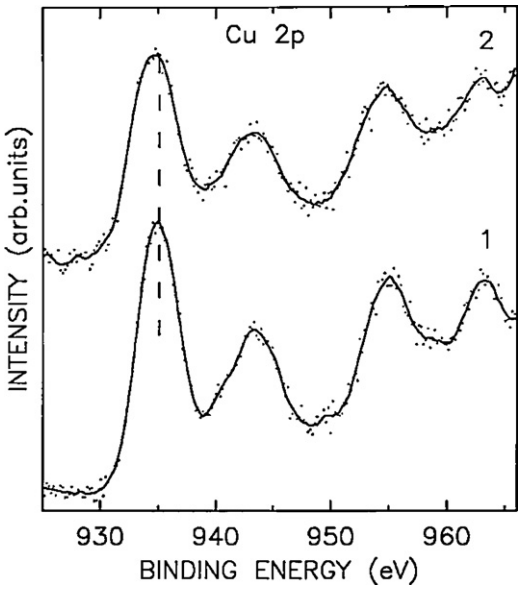

Fig. 3. Spectra of Cu (2p) photoelectrons taken from the samples: (1) Cu-py-ZSM5 (L) and (2) Cu-py-CT (L).

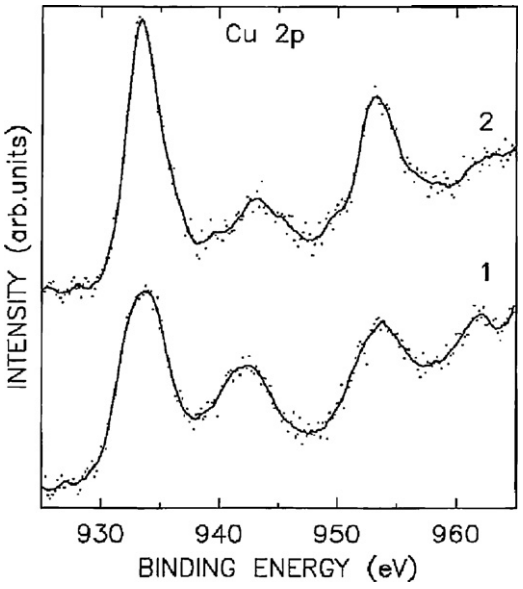

Fig. 4. Spectra of Cu (2p) photoelectrons taken from the sample Cu-py-CT (L). The spectrum 2 was measured 140 min after acquisition of the spectrum 1. During this time period the sample was irradiated by X-ray radiation used to excite electrons.

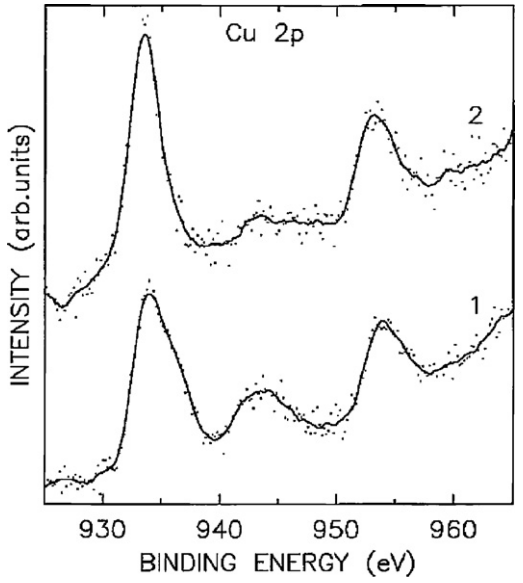

Fig. 5. Spectra of Cu (2p) photoelectrons taken from the sample Cu-CT. The spectrum 2 was measured 140 min after acquisition of the spectrum 1. During this time period the sample was irradiated by X-ray radiation used to excite electrons.

3.2. IR spectroscopy

IR spectra of the starting zeolitic samples Cu-ZSM5, Cu-CT as well as the samples after the sorption of pyridine were taken. The presence of pyridine was confirmed in the samples Cu-py-ZSM5 and Cu-py-CT. In the studied region (400–4000 cm^{-1}) several peaks can be observed that were attributed to the stretching vibrations of OH groups affiliated with tetrahedrally coordinated aluminium (3606–3609 cm^{-1}) and water (3446–3450 cm^{-1}), deformation vibration of water at 1640 cm^{-1}, stretching vibrations of Si–O groups (1052–1059 cm^{-1}), deformation vibrations of OH groups (789–798 cm^{-1}), deformation vibrations of Al–O–Si groups at 547 cm^{-1} and Si–O–Si at 444–454 cm^{-1}. The results are in a good agreement with the literature [29–31]. The spectra of zeolitic samples containing pyridine show the ring vibration of pyridine detected in the frequency range of 1400–1650 cm^{-1} (Fig. 7) commonly used to characterize the concentrations of Brönsted and Lewis acid sites [31–33]. The Brönsted acid sites correspond to the 1545 cm^{-1} band (pyridinium ion). The Lewis acid sites give rise to the 1450 cm^{-1} band attributed to pyridine coordinatively bound to accessible Al^{3+}, while the band at 1490 cm^{-1} is attributed to the adsorbed pyridine species on both Brönsted and Lewis acid sites. The absorption of the Al^{3+} band interferes with copper absorption band. Cu-ZSM5 shows only one peak at 1635 cm^{-1} assigned to the deformation vibration of H–O–H groups, but the modified pyridine containing forms exhibit in this region two absorption bands that partially interfere at 1609–1635 cm^{-1} (a pure pyridine exhibits a peak at 1583 cm^{-1} in the studied region [34]). It has been proved [35–37] that these peaks of pure ligands shift to the higher frequencies upon a complex formation. The shift of the experimentally obtained peaks to about 1608 cm^{-1} (py) may support the conclusion concerning a formation of the coordinate bond between copper ions and the nitrogen atom of heterocyclic ring. This assertion is also supported by the presence of the diagnostic Lewis peak at ≈1435–1450 cm^{-1}.

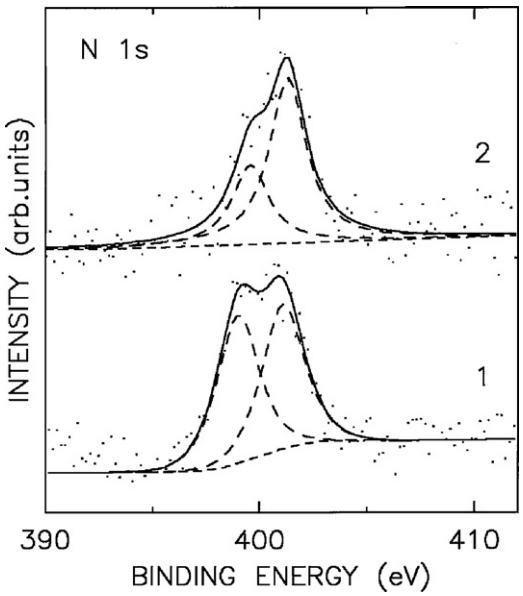

Fig. 6. Fitted spectra of N (1s) photoelectrons: (1) Cu-py-ZSM5 (L) and (2) Cu-py-CT (L).

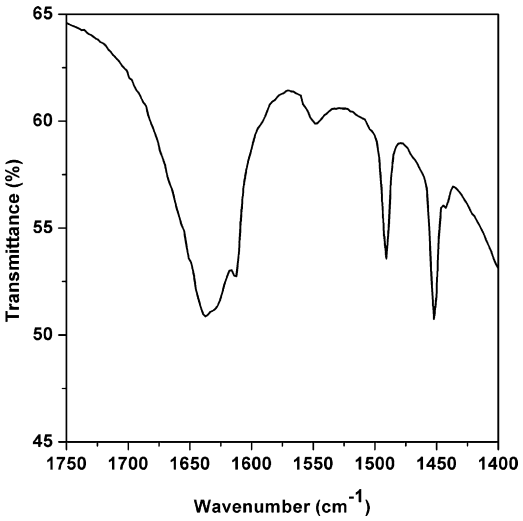

Fig. 7. IR spectrum of Cu-py-ZSM5 (L) in the range from 1750 to 1400 cm^{-1}.

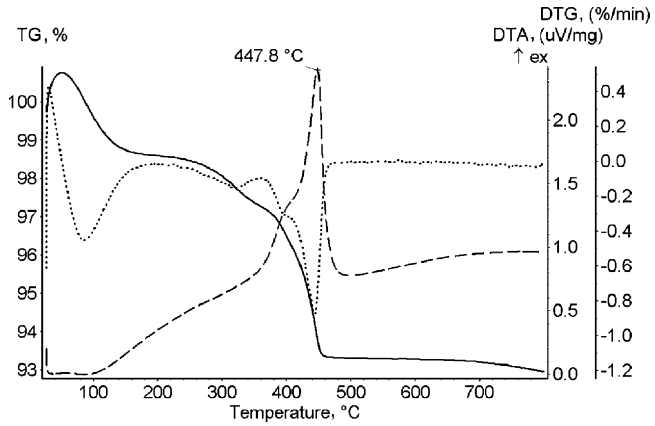

Fig. 8. TG (—), DTG (···) and DTA (- - -) curves of the sample Cu-py-ZSM (L).

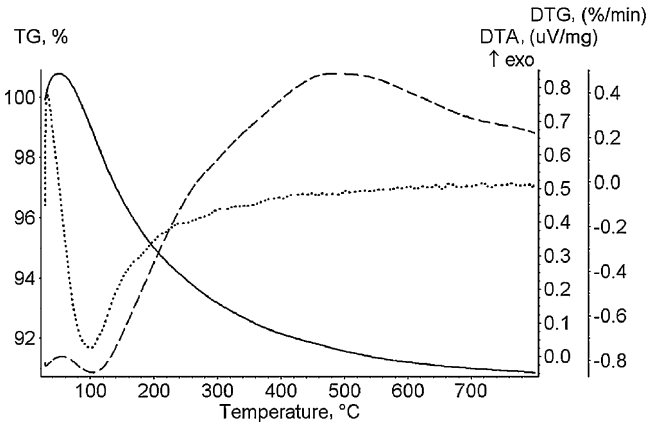

Fig. 10. TG (—), DTG (···) and DTA (- - -) curves of the sample Cu-CT.

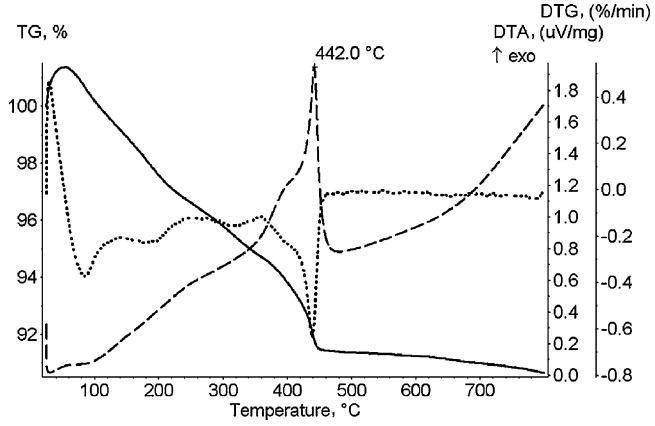

Fig. 9. TG (—), DTG (···) and DTA (- - -) curves of the sample Cu-py-ZSM5 (G).

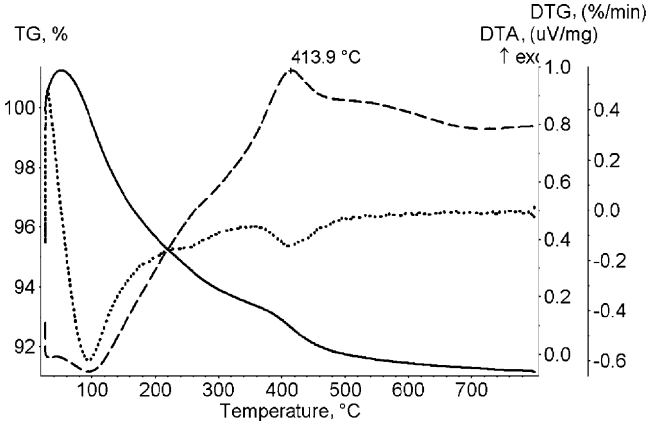

Fig. 11. TG (—), DTG (···) and DTA (- - -) curves of the sample Cu-py-CT (G).

To better resolve the pyridine release, IR measurements of intermediate products of thermal decomposition of the sample Cu-py-ZSM5 (L) at temperatures 150, 200, 250, 300, 350, 400 and 450 °C were performed. The presence of pyridine was confirmed in IR spectra of all intermediate products obtained from 150 °C to 400 °C, however, in the IR spectra of the intermediate product obtained after the heating at 450 °C the vibrations of pyridine were missing. These results are in a good agreement with the results of thermal analysis (Fig. 8).

3.3. Thermal analysis

The methods of thermal analysis significantly contributed to the characterization of the sorption processes of pyridine by copper forms of synthetic and natural zeolites and to the better specification of the interaction between pyridine and the zeolitic structure.

The results of thermal analyses clearly show different properties of two solids: starting zeosorbents Cu-ZSM5, Cu-CT and zeosorbents containing pyridine Cu-py-ZSM5 and Cu-py-CT (Figs. 8–11). The products containing pyridine have different TG, DTG and DTA curve in comparison with the starting copper forms Cu-ZSM5 and Cu-CT. The results of thermal analysis obtained for Cu-ZSM5 samples were reported in our previous paper [25].

During thermal analysis of Cu-py-ZSM5 (L), in the first endothermic process up to the temperature 150 °C water is released (1.2%). The exothermic process in the temperature range 150–460 °C corresponds to pyridine release (5.5%) in three steps (Fig. 8): the first step in temperature range from 150 °C to 340 °C, the second one from 340 °C to 400 °C, the third one up to temperature 450 °C with a maximum of the strong exothermic peak on the DTA curve at 447.8 °C and with a clear weight loss on the TG curve. It can be assumed that the release of the pyridine in the third step refers to pyridine coordinated to copper ions. Thermal analysis of the sample Cu-py-CT (L) confirmed the release of pyridine, too. On the DTA curve we can see endothermic process up to the temperature 200 °C and exothermic process in the temperature range 200–480 °C with a maximum at 437.1 °C which corresponds to a weight loss on the TG curve. A small peak on the DTG curve in the temperature range 200–300 °C appears, too. The content of adsorbed pyridine is lower in comparison with the sample Cu-py-ZSM5 (L), consequently, the peaks on the DTG curve are not so intensive.

In the samples obtained by the sorption of pyridine from the gas phase (Figs. 9 and 11) Cu-py-ZSM5 (G) and Cu-py-CT (G), the desorption of a part of pyridine starts at lower temperatures (together with water) as compared with the samples Cu-py-ZSM5 (L) obtained from liquid phase.

It si known from the literature [33,38] that during thermal analysis pyridine is released in several steps from Brönsted and Lewis sites.

The main part of the pyridine is released from the products Cu-py-ZSM5 and Cu-py-CT at remarkably higher temperatures than is the boiling point of pyridine (115.2 °C). It provides evidence in favour of "strong" bond and irreversible interaction of the py–zeolite. The main part of pyridine is chemisorbed on Brönsted and Lewis acid sites. In the case of the samples Cu-py-ZSM5 (G) and Cu-py-CT (G), which were obtained by the sorption of pyridine from

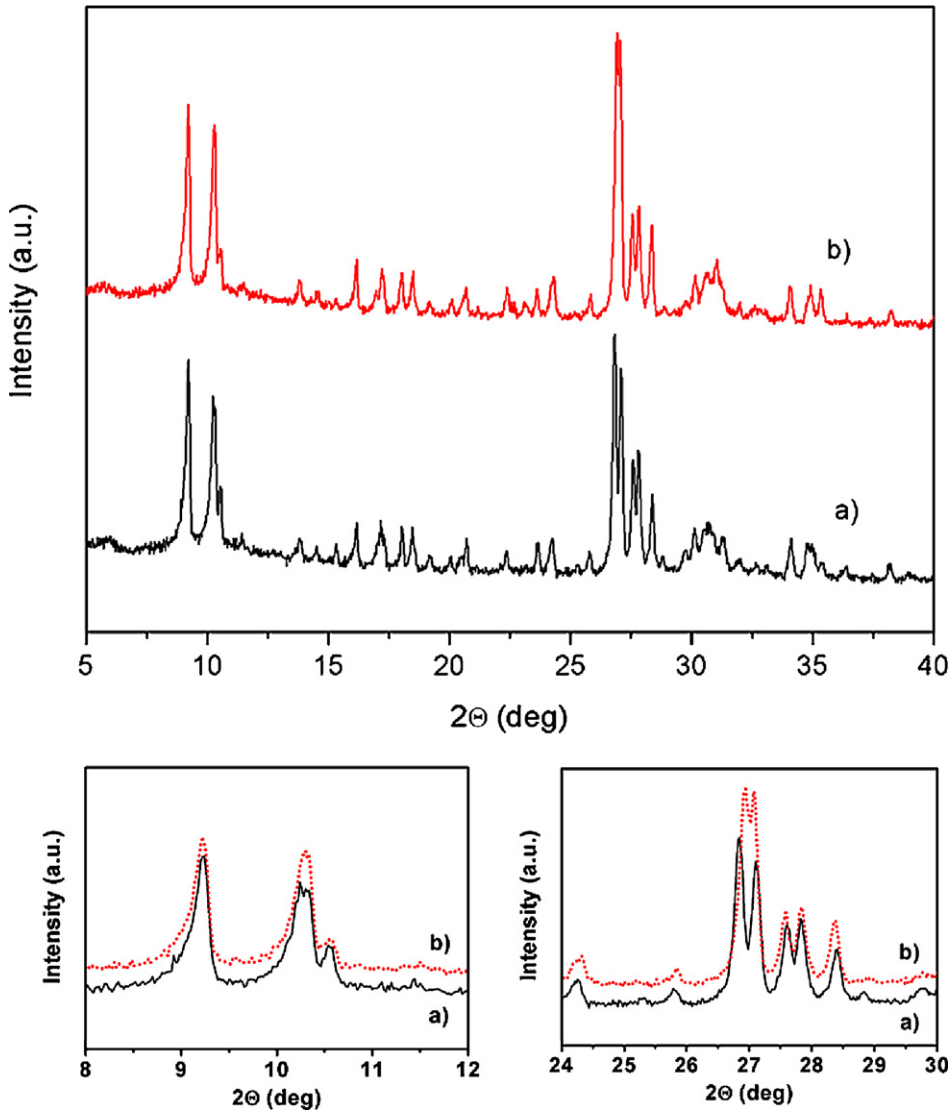

Fig. 12. The X-ray diffraction patterns of Cu-ZSM5 (a) and Cu-py-ZSM5 (b).

the gas phase, however, a small amount of physisorbed pyridine is released from the samples at lower temperature, together with water. Physically adsorbed pyridine on synthetic zeolites (ZSM5, ZSM2 and H-β zeolites) in the temperature range from 100 to 150 °C was reported also in other studies [33,39–41]. Chemisorption of pyridine on synthetic zeolites is known from literature [33,42,43].

To obtain more information about thermal decomposition of the samples Cu-py-ZSM5 and Cu-py-CT, mainly those concerning the decomposition products of thermal analysis, it would be necessary to analyse the decomposition products by mass spectroscopy, too. The previous studies of thermal decomposition of copper forms of synthetic zeolite ZSM5 containing organic diamines (ethylenediamine and dimethylethylenediamine) confirmed that, as a consequence of the catalytic effect of the silicate surface, condensation and polymerisation reactions of the primarily released products occur [44,45]. In case of the study of copper forms of synthetic zeolite ZSM5 and natural clinoptilolite with pyridine content, oxidation (in air atmosphere) of the released pyridine during exothermic process of thermal analysis [46] occurs as well as other reactions of the released products as a result of the catalytic effect of the silicate surface may occur.

3.4. X-ray diffraction analysis

In Fig. 12, X-ray diffraction patterns of the samples Cu-ZSM5, Cu-py-ZSM5 (L) and selected regions of peaks at $2\theta = 8–12^\circ$ and $24–30^\circ$ can be seen, which correspond to the specific peaks of ZSM5 zeolite [47,48]. The selected regions show that the characteristic peaks for Cu-exchanged zeolites are similar to those of pure ZSM5. No significant diffraction lines which could be assigned to any new phase, as are extra-framework pyridine complexes of Cu, are observed. Moreover, there is a shift in the peak positions at about 27° 2θ which indicates changes in the nature of the cations and their distribution due to the formation of complex Cu-py cations in intra-framework spaces of zeolite. The integral intensity ratio of selected diffraction line of Cu-ZSM5 and Cu-py-ZSM5 in the range of $2\theta = 9.5–11^\circ$ and $26–29^\circ$ shows also a small difference. It can be concluded that pyridine is included in intra-framework spaces of synthetic zeolite ZSM5.

3.5. Analysis of the surface areas and the pore volumes

The results of the study of the surface area changes of the zeolitic samples are shown in Fig. 13 and are in a good agreement with the

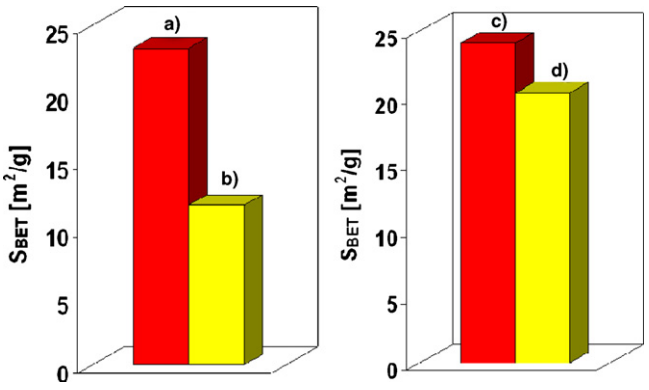

Fig. 13. Diagram of surface area S_{BET} [m^2/g] of copper zeolitic samples and after adsorption of pyridine: (a) Cu-ZSM5, (b) Cu-py-ZSM5 (L), (c) Cu-CT and (d) Cu-py-CT (L).

Table 3
The surface areas (S_{BET}) and pore volumes of the studied zeolitic samples.

Sample	S_{BET} [m^2/g]	Pore volume [cm^3/g]
Cu-ZSM5	23.3619	0.0375
Cu-py-ZSM5 (L)	11.8035	0.0168
Cu-py-ZSM5 (G)	11.0191	0.0156
Cu-CT	23.9645	0.0384
Cu-py-CT (L)	20.8700	0.0354
Cu-py-CT (G)	20.3243	0.0211

results of the pore volumes measurement (Table 3). By the comparison of the results for the starting copper zeolitic samples and the samples after the sorption of pyridine, it was found that the surface areas and pore volumes decreased due to the adsorption of pyridine. The surface areas and pore volumes of the starting samples are relatively low because, before the measurements, all samples were heated only to the temperature 105 °C for 2 h. Higher temperatures in order to remove water could not be applied since the desorption of pyridine could already occur.

4. Conclusion

For the sorption of toxic pyridine from the liquid and gas phase, the zeosorbents on the bases of copper forms of synthetic zeolite ZSM5 and natural zeolites of the clinoptilolite type were used. The methods of thermal analysis and FTIR significantly contributed to a more detailed characterization of the sorption processes of pyridine by copper forms of synthetic and natural zeolites. The content of the sorbed pyridine in zeosorbents was different and dependent on the experimental conditions during the preparation of the modified copper forms of synthetic and natural zeosorbents, as well as during the sorption process. An increase in the amount of sorbed pyridine by following modification of the zeosorbents can be possible. NMR spectroscopy studies of the zeosorbents after pyridine sorption will be applied in order to better understanding the sorption process and the interaction of pyridine with zeolitic structure.

The copper forms of zeosorbents have been studied for their environmental application in the field of removing harmful pyridine. In combination with a following biodegradation of pyridine, using a metabolic activity of some microorganisms, it could be a perspective ecological alternation of degradation of the pyridine contaminants.

Acknowledgements

Three of the authors gratefully acknowledge the financial support provided by the Scientific Grant Agency of the Slovak Republic (grant no. 1/0107/08). One of the authors (Z.B.) thanks to the Grant Agency of Academy of Sciences of the Czech Republic (grant no. KAN 100400702).

References

[1] J. Li, W. Cai, J. Cai, The characteristics and mechanisms of pyridine biodegradation by *Streptomyces* sp., J. Hazard. Mater. 165 (2009) 950–954.
[2] L. Qiao, J. Wang, Microbial degradation of pyridine by *Paracoccus* sp. isolated from contaminated soil, J. Hazard. Mater. 176 (2010) 220–225.
[3] A.K. Mathur, C.B. Majumder, S. Chatterjee, P. Roy, Biodegradation of pyridine by the new bacterial isolates *S. putrefaciens* and *B. sphaericus*, J. Hazard. Mater. 157 (2008) 335–343.
[4] D.J. Richards, W.K. Shieth, Biological fate of organic priority pollutants in the aquatic environment, Water Res. 20 (1986) 1077–1090.
[5] C. Zhang, M. Li, G. Liu, H. Luo, R. Zhang, Pyridine degradation in the microbial fuel cells, J. Hazard. Mater. 172 (2009) 465–471.
[6] D.H. Lataye, I.M. Mishra, I.D. Mall, Removal of pyridine from aqueous solution by adsorption on bagasse fly ash, Ind. Eng. Chem. Res. 45 (2006) 3934–3943.
[7] D. Mohan, K.P. Singh, S. Sinha, D. Gosh, Removal of pyridine from aqueous solution using low cost activated carbons derived from agricultural waste materials, Carbon 42 (2004) 2409–2421.
[8] K.V. Padoley, A.S. Rajvaidya, T.V. Subbarao, R.A. Pandey, Biodegradation of pyridine in a completely mixed activated sludge process, Bioresour. Technol. 97 (2006) 1225–1236.
[9] S. Fetzner, Bacterial degradation of pyridine, indole, quinoline and their derivatives under different redox conditions, Appl. Microbiol. Biotechnol. 49 (1998) 237–250.
[10] S.T. Lee, T.K. Rhee, G.M. Lee, Biodegradation of pyridine by freely suspended and immobilized *Pimelobacter* sp., Appl. Environ. Microbiol. 41 (1994) 652–657.
[11] M.A. Stylianou, M.P. Hadjiconstantinou, V.J. Inglezakis, K.G. Moustakas, M.D. Loizidou, Use of natural clinoptilolite for the removal lead, copper and zinc in fixed bed column, J. Hazard. Mater. 143 (2007) 575–581.
[12] M. Reháková, S. Čuvanová, M. Dzivák, J. Rimár, Z. Gaval'ová, Agricultural and agrochemical uses of natural zeolite of the clinoptilolite type, Curr. Opin. Solid State Mater. 8 (2004) 397–404.
[13] E. Chmielewská, K. Pilchowski, Surface modifications of natural clinoptilolite-dominated zeolite for phenolic pollutant mitigation, Chem. Pap. 60 (2006) 98–101.
[14] W.T. Tsai, K.J. Hsien, H.C. Hsu, Adsorption of organic compounds from aqueous solution onto the synthesized zeolite, J. Hazard. Mater. 166 (2009) 635–641.
[15] W. Shi, H. Shao, H. Li, M. Shao, S. Du, Progress in the remediation of hazardous heavy metal-polluted soils by natural zeolite, J. Hazard. Mater. 170 (2009) 1–6.
[16] H. Li, W. Shi, H. Shao, M. Shao, The remediation of the lead-polluted garden soil by natural zeolite, J. Hazard. Mater. 169 (2009) 1106–1111.
[17] P. Chutia, S. Kato, T. Kojima, S. Satokawa, Arsenic adsorption from aqueous solution on synthetic zeolites, J. Hazard. Mater. 162 (2009) 440–449.
[18] B. Gennaro, A. Colella, P. Cappelletti, M. Pansini, M. Gennaro, C. Colella, Effectiveness of clinoptilolite in removing toxic cations from water: a comparative study, in: J. Čejka, N. Žilková, P. Nachtigall (Eds.), Studies in Surface Science and Catalysis, vol. 158, Elsevier, Amsterdam, 2005, pp. 1153–1160.
[19] M. Reháková, A. Sopková, M. Casciola, Z. Bastl, Ac and dc conductivity study of natural zeoitic material of the clinoptilolite type and its iodine forms, Solid State Ionics 66 (1993) 189–194.
[20] M. Reháková, Z. Bastl, P. Finocchiaro, A. Sopková, X-ray photoelectron spectroscopic studies of a iodine doped natural zeolite of clinoptilolite type and its thermally degraded products, J. Therm. Anal. 45 (1995) 511–518.
[21] D.A. Shirley, High resolution X-ray photoemission spectrum of the valence bands of Au, Phys. Rev. 85 (1972) 4709–4714.
[22] J.H. Scofield, Hartree–Slater subshell photoionization cross-sections at 1254 and 1487 eV, J. Electron Spectrosc. Relat. Phenom. 8 (1976) 129–137.
[23] M.P. Seah, in: D. Briggs, M.P. Seah (Eds.), Practical Surface Analysis, vol. 1, Wiley, Chichester, 1990, pp. 201–255.
[24] M.P. Seah, W.A. Dench, Quantitative electron spectroscopy of surfaces: a standard data base for electron inelastic mean free paths in solids, Surf. Interface Anal. 1 (1979) 2–11.
[25] M. Reháková, T. Wadsten, S. Nagyová, Z. Bastl, J. Briančin, Study of copper forms of the synthetic zeolite ZSM5 containing ethylenediamine, J. Incl. Phenom. 39 (2001) 181–186.
[26] G. Moretti, G. Minelli, P. Porta, P. Ciambeli, P. Corbo, XPS and adsorption of dinitrogen studies on copper-ion exchanged ZSM-5 and Y zeolites, in: H.G. Karge, J. Weitkamp (Eds.), Studies in Surface Science and Catalysis, vol. 98, Elsevier, Amsterdam, 1995, pp. 69–70.
[27] R. Borade, A. Adnot, S. Kaliaguine, An XPS study of acid sites in dehydroxylated Y zeolites, J. Mol. Catal. 61 (1990) 7–14.
[28] R. Borade, A. Sayrai, A. Adnot, S. Kaliaguine, Characterization of acidity in ZSM-5 Zeolites: an X-ray photoelectron and IR spectroscopy study, J. Phys. Chem. 94 (1990) 5989–5994.
[29] K.S. Smirnov, D. Bougeard, Computer modeling of the infrared spectra of zeolite catalysts, Catal. Today 70 (2001) 243–253.

[30] J. Datka, B. Gil, P. Baran, Heterogeneity of OH groups in HZSM-5 zeolites: splitting of OH and OD bands in low-temperature IR spectra, Micropor. Mesopor. Mater. 58 (2003) 291–294.
[31] J.A. Lercher, A. Jentys, Infrared and Raman spectroscopy for characterizing zeolites, in: J. Čejka, H. van Bekkum, A. Corma, F. Schüth (Eds.), Studies in Surface Science and Catalysis, vol. 168, Third ed., Elsevier, Amsterdam, 2007, pp. 435–476.
[32] B. Gil, Acidity of zeolites, in: J. Čejka, J. Peréz-Pariente, W.J. Roth (Eds.), Zeolites: From Model Materials to Industrial Catalysts, Transworld Research Network, Trivandrum, 2008, pp. 173–206.
[33] F. Jin, Y. Li, A FTIR and TPD examination of the distributive properties of acid sites on ZSM-5 zeolite with pyridine as a probe molecule, Catal. Today 145 (2009) 101–107.
[34] J.H.S. Green, W. Kynaston, H.M. Paisley, Vibrational spectra of monosubstituted pyridines, Spectrochim. Acta 19 (1963) 549–564.
[35] S.C. Mojumdar, Processing-moisture resistance and thermal analysis of macro-defect-free materials, J. Therm. Anal. Calorim. 64 (2001) 629–636.
[36] E. Jóna, E. Rudinská, M. Kubranová, M. Sapietová, M. Pajtášová, V. Jorík, Intercalation of pyridine derivatives and complex formation in the interlayer space of Cu(II)-montmorillonite, Chem. Pap. 59 (2005) 248–250.
[37] S.C. Mojumdar, M. Melník, Preparation, spectral and thermal properties of Mg(II) and Cu(II) complexes with N,N-diethylnicotinamide, Chem. Pap. 54 (2000) 1–5.
[38] R. Burch, C. Howitt, Investigation of zeolite catalysts for the direct partial oxidation of benzene to phenol, Appl. Catal. 103 (1993) 135–162.
[39] A. Tamási, I. Kiricsi, Z. Kónya, J. Halász, L. Guczi, Infrared spectroscopic studies on the surface chemistry of bimetallic zeolite systems. Acidity of Pt,Co- and Pt,CuZSM-5 zeolites, J. Mol. Struct. 482–483 (1999) 1–5.
[40] C. Covarrubias, R. Quijada, R. Rojas, Synthesis of nanosized ZSM-2 zeolite with potential acid catalytic properties, Micropor. Mesopor. Mater. 117 (2009) 118–125.
[41] M. Maache, A. Janin, J.C. Lavalley, J.F. Joly, E. Benazzi, Acidity of zeolites beta dealuminated by acid leaching: an FTIR study using different probe molecules (pyridine, carbon monooxide), Zeolites 13 (1993) 419–426.
[42] V.R. Choudhary, A.K. Kinage, C. Sivadinarayana, M. Guisnet, Influence of O_2 and H_2 pretreatments on acidity/acid strength distribution and acid functions of Ga/H-ZSM5, H-GaMFI and H-GaAl MFI zeolites, Proc. Indian Acad. Sci. (Chem. Sci.) 108 (1996) 89–100.
[43] V.R. Choudhary, V.S. Nayak, Chemisorption and temperature programmed desorption of pyridine on H-ZSM-5 zeolites, Mater. Chem. Phys. 11 (1984) 515–523.
[44] M. Reháková, K. Jesenák, S. Nagyová, R. Kubinec, S. Čuvanová, V.Š. Fajnor, Thermochemical properties of copper forms of zeolite ZSM5 containing ethylenediamine, J. Therm. Anal. Calorim. 76 (2004) 139–147.
[45] S. Čuvanová, M. Reháková, P. Finocchiaro, A. Pollicino, Z. Bastl, S. Nagyová, V.Š. Fajnor, Thermochemical properties of copper forms of zeolite ZSM5 containing dimethylethylenediamine, Thermochim. Acta 452 (2007) 13–19.
[46] S. Yariv, The role of charcoal on DTA curves of organo-clay complexes: an overview, Appl. Clay Sci. 24 (2004) 225–236.
[47] Y. Cheng, L.J. Wang, L.S. Li, Y.C. Yang, X.Y. Sun, Preparation and characterization of nanosized ZSM-5 zeolites in the absence of organic template, Mater. Lett. 59 (2005) 3427–3430.
[48] M.C. Dalconi, G. Cruciani, A. Alberti, P. Ciambelli, Over-loaded Cu-ZSM-5 upon heating treatment: a time resolved X-ray diffraction study, Micropor. Mesopor. Mater. 94 (2006) 139–147.